Simulation Analysis of Intelligent Control System for Excavators in Large Mining Plants Based on Electronic Control Technology

Lei Sun
School of Intelligent Manufacturing, Shandong Polytechnic, Ji'nan, 250000, China

***Abstract*—With the increasing demand for large-scale mine equipment and the complexity of the operating environment, the intelligent trajectory planning and control of mine systems becomes very important. This paper proposes a proportional-integral-differential (PID) feedback controller combined with adaptive improvement. This controller combines Genetic Algorithm and Particle Swarm Optimization technology to enhance the ability of the excavator's intelligent control system and improve the control accuracy, response speed, and robustness under different working conditions. The results showed that the constructed PID controller improved the average constraint performance by 2.5% through quintic interpolation, and the power consumption was relatively small. The trajectory prediction error of different joints was less than 5% and the displacement and pressure curves of the hydraulic cylinder were stable and symmetrical. The accuracy of the proposed algorithm was 94% and quickly converged to 0.05 after 50 iterations, which was 18.5%, 15.3%, and 17.5% higher than the other three algorithms, respectively. Therefore, the proposed method has high reliability and adaptability in anti-interference ability, trajectory planning progress, and optimization efficiency, and it provides a better solution for intelligent control of the excavator excavation system.**

***Keywords*—Genetic Algorithm; Particle Swarm Optimization; proportional-integral-differential; mining system; intelligent control**

I. Introduction

As global demand for mineral resources continues to rise, the existing production efficiency of the mining industry is unable to meet the current consumption needs. Furthermore, the safety of mining workers and the costs associated with production are also pressing concerns that require immediate attention [1]. Excavators represent the core equipment of large mining plants. However, they currently face significant challenges, including difficulties in dealing with complex mining environments, a lack of flexibility, and a lack of intelligent control [2]. The advancement of Electronic Control Technology (ECT) has provided the possibility for the emergence of Intelligent Control Systems (ICS) for excavators, which can to some extent meet the operational needs of large-scale mining industries. Currently, experts have extensively researched excavator ICS and algorithm optimization [3]. However, the existing excavators have obvious shortcomings in dealing with the changing mine environment, improving operation accuracy, and enhancing intelligent control. To solve these problems, this study proposes an ICS based on ECT to improve the performance of excavators in complex mine environments through advanced control strategies. The innovation of the research lies in the development of a Proportional-Integral-Differential (PID) controller, which combines Genetic Algorithm (GA) and Particle Swarm Optimization (PSO) technology to enhance the adaptability and robustness of the excavator ICS. Through this combined optimization strategy, this method not only improves the control accuracy and response speed but also improves the anti-interference ability of the system in the face of internal and external interference.

This study proposes a PID feedback controller combining GA and PSO technology to improve the ICS performance of large mining excavators. By adopting the PID controller and GA-PSO optimization strategy, the control accuracy and response speed of ICS are improved. Compared with the existing PID control technology, fuzzy control, and GA and PSO when employed in isolation, the improved PID feedback control method combined with GA-PSO has stronger comprehensive performance in search performance and convergence speed and realizes more effective trajectory optimization.

The overall structure of the study includes six sections. Introduction is given in Section I. Section II summarizes the research achievements and shortcomings of ECT in ICS of different countries. The second section studies and designs the simulation model of PID feedback control. Section III tests and analyzes the proposed model. Section IV discusses the experimental results. Discussion is given in Section V and finally, Section VI concluded the paper.

II. Related Works

Significant progress has been made in the application of ECT in excavator ICS [4-5]. Sadiq et al. put forth a PID-Mining Control Systems (MCS) method based on adaptive adjustment, which was designed to address the issue that traditional MCSs are unable to effectively address the influence of nonlinear factors. This method could improve the control performance of load fluctuations. This method has reduced the response time by 13% compared to the PID control technology before improvement [6]. Wellendorf et al. designed a PSO-based PID control parameter optimization method to address the issue of traditional MCS relying on manual experience. It has improved stability by 20% compared to traditional control systems [7]. Kanso et al. proposed an adaptive PID control method based on fuzzy logic to address the limitations of traditional manual experience-based control of mining systems. This method reduced the response time by 14% and improved its robustness

by 34% [8]. Wang Z et al. proposed a PID control technique grounded on Deep Learning (DL) algorithms. The DL and predictive capabilities of this algorithm have improved the accuracy and response speed by 23% and 12%, respectively [9]. Sohail A et al. proposed a mining job scheduling optimization method based on an ant colony algorithm. Compared to traditional control systems, this method has increased mining efficiency by 28% and resource utilization by 10% [10].

The trajectory planning control method based on GA and PSO algorithms has also received widespread attention [11]. Gad et al. proposed a GA-based path optimization scheme for trajectory planning problems in complex environments. This method could obtain the global Optimal Solution (OS) under complex road conditions [12]. Pervaiz et al. developed an approach that simulates the objective function of PSO and updates the position and velocity of particles to obtain the OS, which has a fast convergence performance [13]. Zhang et al. established a trajectory planning control method based on GA-PSO, which expands the search range through crossover and mutation, and locally refines with PSO, significantly improving the accuracy and efficiency of the algorithm [14]. Minh et al. suggested a multi-objective optimization method fused with GA-PSO for nonlinear factors in complex environments. This method utilized the OS and hierarchical selection mechanism to achieve the OS under multi-objective common constraints [15]. Pozna et al. proposed a GA-PSO that combines DL and the feature extraction capability of DL to predict the priority of trajectory points, improving the intelligence level of path planning. This method could be used for path planning in complex environments and ensure the stability and reliability of the results [16].

In summary, existing research has made certain progress in anti-interference and trajectory optimization [17]. However, in more complex large-scale mining environments, the comprehensive control performance of the method still needs improvement, with limitations in response speed, control accuracy, anti-interference ability, and robustness [18-19]. Therefore, this study proposes an ECT-based ICS for large mining plant excavators to enhance their overall performance and control capabilities in complex working conditions. The innovation of the research lies in proposing a PID anti-interference control model based on adaptive improvement, aiming to improve the internal and external anti-interference performance of the algorithm. The trajectory control model combined with the GA-PSO optimization algorithm can improve the optimization of global and local solutions in complex and real-world environments while ensuring the accuracy and efficiency of the solutions. This study provides a better solution for excavator trajectory planning.

III. Methods and Materials

The first section constructs an anti-interference mining system. Firstly, a mechanical arm simulation dynamic model based on improved D-H parameters is established, and forward and inverse dynamics verification is carried out. Finally, a PID controller is introduced to further optimize the control performance of the mining trajectory planning system. The second section introduces the GA-PSO algorithm to optimize the parameters of the PID controller, further enhancing the control performance of the mining system.

A. Construction of PID Feedback Control Simulation Model for Anti-Interference Mining System

The operating environment of large mining plants is complex and harsh. The operation of excavators is inevitably limited by environmental factors, and it is also necessary to deal with self-interference caused by factors such as inertia and vibration during the excavator's movement process [20-21]. To enhance the ability of mining systems to cope with complex environments, it is necessary to construct a PID feedback control simulation model based on mining systems for trajectory planning and control. This study first establishes a geometric simulation model of the Robotic Arm (RA), defining the length, mass, centroid position, and inertia tensor of the joints and linkages of the RA. Subsequently, based on the improved D-H parameters, a coordinate for the linkage of the excavator arm is established, as shown in Fig. 1 [22-23].

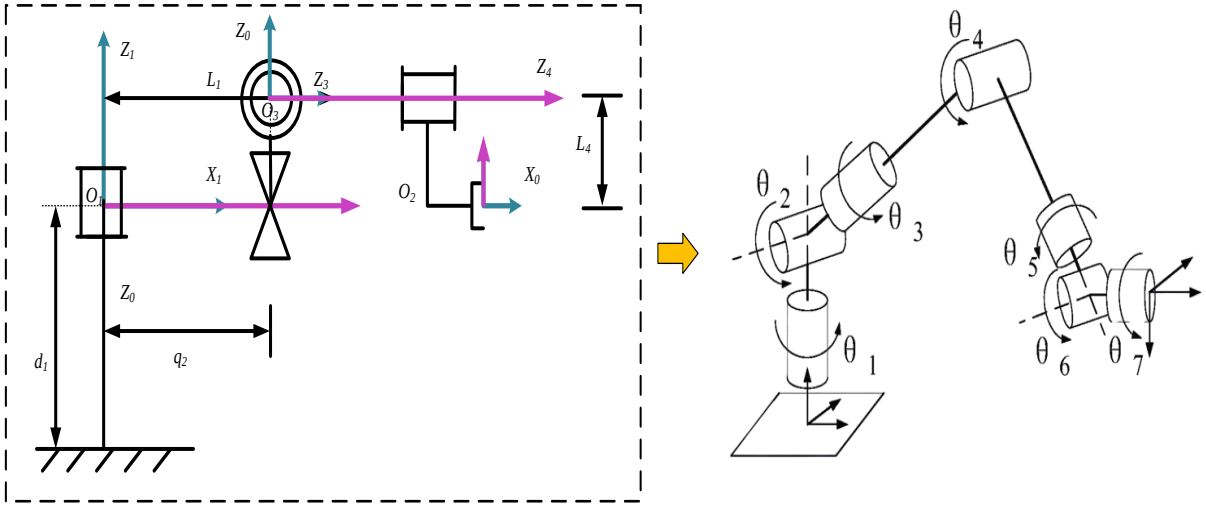

Fig. 1. Structural diagram of the coordinate system of the RA.

Based on the improved D-H parameters, each joint angle and link length of the RA is defined, and a coordinate system is set for each joint to determine the relationship between the joints. A positive dynamics verification is conducted on the constructed geometric simulation model of the RA, thereby obtaining the relationship between the posture and joint angles of the end position of the RA. The homogeneous transformation matrix between the connecting rod and the joint is shown in Eq. (1).

$$ {}_{i}^{i-1}\boldsymbol{T} = \begin{bmatrix} \cos\theta_i & -\sin\theta_i\cos\alpha_i & \sin\theta_i\sin\alpha_i & a_i\cos\theta_i \\ \sin\theta_i & \cos\theta_i\cos\alpha_i & -\cos\theta_i\sin\alpha_i & a_i\sin\theta_i \\ 0 & \sin\alpha_i & \cos\alpha_i & d_i \\ 0 & 0 & 0 & 1 \end{bmatrix} \quad (1) $$

In Eq. (1), ${}_{i}^{i-1}\boldsymbol{T}$ is the transformation relationship between adjacent linkage coordinate systems i and $i-1$. θ_i is the angle of rotation required for the connecting rod connecting two adjacent joints. α_i and d_i are the other angle and displacement length required to connect two adjacent joints. a_i is the horizontal distance between adjacent joints. The transformation matrix effectively describes the directional relationship between each joint and link in the structure of the RA, which can be used to obtain the final posture of the RA and accurately describe the pose of the RA at specific time points during motion. Using MATLAB for inverse dynamics verification, a simulation model is constructed to obtain the motion parameters of the RA. To ensure the accuracy of the excavator during excavation, handling, and movement in complex mining environments, the interpolation method is utilized to simulate the motion process multiple times. The motion parameters of the RA are obtained at each moment and then adjusted to ensure the model's accuracy. To ensure both the economy and stability of the RA control process, a Five Order Interpolation Method (FOIM) is adopted, as shown in Eq. (2).

$$ \theta(t) = A_0 + A_1 t + A_2 t^2 + A_3 t^3 + A_4 t^4 + A_3 t^5 \quad (2) $$

In Eq. (2), $\theta(t)$ is the rotation angle of the RA joint at time t. A_0, A_1, A_2, A_3, A_4, and A_5 are the difference coefficients related to t, representing the positions of each joint of the RA at time t. Through FOIM, more accurate simulation results of the RA are obtained. To further obtain a more optimal robot motion path and determine the objective function, the parameters during the movement of the RA are adjusted to ensure that the path meets the requirements, as given by Eq. (3).

$$ F(x) = \alpha f_1(x) + \beta f_2(x) \quad (3) $$

In Eq. (3), α and β are weighting coefficients. $F(x)$ is the objective function for the optimal path of the RA. $f_1(x)$ is a matrix constraint condition that describes the range of motion space of the RA. $f_2(x)$ is the proportion of the RA in the workspace. Considering the influence of factors such as gravity and inertia during the movement of the RA, this study presents challenges for precise control and efficient operation of the motion. Therefore, the derived joint torque is shown in Eq. (4).

$$ \tau = M(q)q + V(q,q) + G(q) \quad (4) $$

In Eq. (4), τ is the joint torque of the RA. $M(q)$ is the inertia matrix of the RA itself. q, q, and q are the joint gravity, inertia, and centripetal force of the RA, respectively. $G(q)$ is the gravity vector of the RA, which describes the influence of gravity on the joints. $V(q,q)$ is the term for centrifugal force and Coriolis force. In complex mining environments, to completely replace manual labor with excavators, it is necessary to ensure the flexibility of excavator movement. The formula for adaptive adjustment of the RA using an anti-interference tracker is given by Eq. (5).

$$ e_1(t) = x_1(t) - z_1(t) \quad (5) $$

In Eq. (5), $e_1(t)$ represents the velocity prediction error value during the motion of the RA. $x_1(t)$ is a nonlinear interference factor. $z_1(t)$ is the true value of the interference factor. To enhance the control capability of the RA over its own interference factors and increase its joint robustness, this study adopts a PID control strategy for the purpose of planning and controlling the motion trajectory of the RA, as illustrated in Fig. 2.

In Fig. 2, the PID controller uses Lyapunov function to perform error control based on the input joint motion state, and updates its motion state to obtain an anti-interference mechanical arm motion process. By using backstepping adaptation, the limitations of the controller can be effectively addressed. The dynamic equation for noise measurement of the sub states of the RA is shown in Eq. (6).

$$ J\,\theta_L = \frac{1}{n}T_m - B\dot{\theta}_L + T_{dis} \quad (6) $$

In Eq. (6), θ_L and θ_L are angular displacement and velocity. J is the gravity vector of the RA joint. T_m is the joint torque input to the PID controller. B is the adaptive control parameter. T_{dis} is the joint torque output by the PID controller. n is the joint variable of the RA. The parameters in the PID controller can be adaptively adjusted based on the influence of environmental and excavator factors. The calculation of parameter adaptive law is shown in Eq. (15).

$$ \hat{\theta} = \Gamma\varphi p \quad (7) $$

In Eq. (7), $\hat{\theta}$ and Γ are the PID control parameter adaptive law and adaptive matrix of the RA. φ is the error between the predicted and actual values of adjacent joint motion sub states. p is the error value of the motion state of the RA.

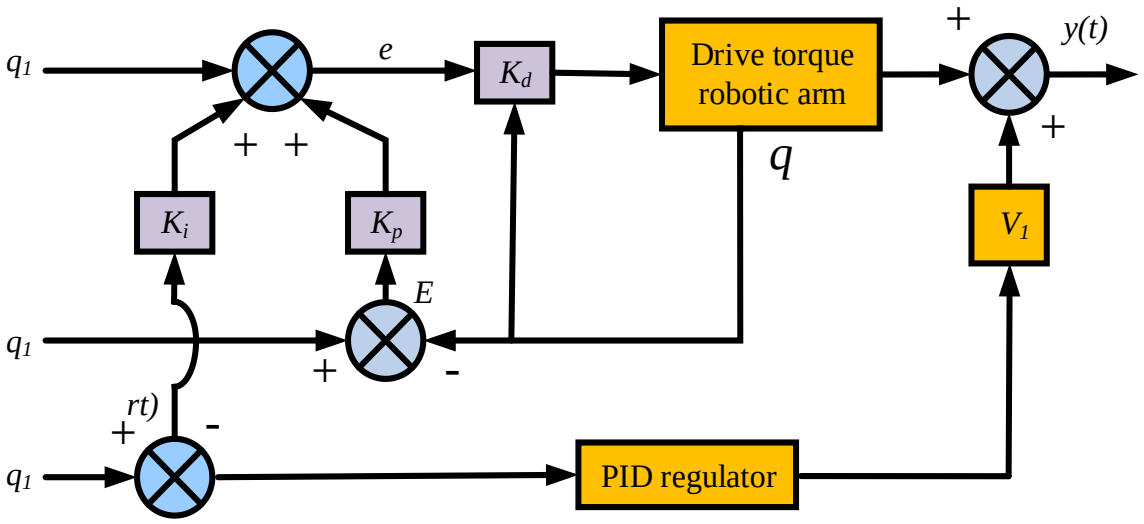

Fig. 2. Schematic diagram of backstepping adaptive control.

B. Construction of Excavator Trajectory Control Model based on GA-PSO

The previous section constructs a mining trajectory planning system based on a PID controller and obtains an anti-interference mechanical arm simulation dynamic model. In the ICS of large mining plants, PID-ECT can achieve excavation trajectory planning and control to enhance the accuracy, efficiency, and flexibility of the excavation process. However, in practical operating environments, due to the complexity of the environment, the feedback control mechanism of PID controllers requires a lot of adjustment time and experience and may encounter problems such as overshoot and oscillation [24-25]. Given these issues, this study proposes a PID control strategy built on GA-PSO to address complex control processes and ensure the accuracy, speed, and robustness of optimal parameter solving. Fig. 3 shows the PID control structure based on the GA-PSO algorithm.

In Fig. 3, GA-PSO searches for the optimal PID parameters to enable the PID controller to provide adjustments for high-frequency and low-frequency signals. GA can search globally by emulating the genetic operations that occur in the natural evolution of organisms. PSO simulates group behavior, and based on the global optimum searched by GA, further performs local fast convergence to obtain more accurate PID parameters. The first step in building GA-PSO is to use GA to randomly generate a set of PID parameters as the initial population, as shown in Eq. (8).

$$u(t) = K_p e(t) + K_i \int e(t)dt + K_d \frac{de(t)}{dt} \tag{8}$$

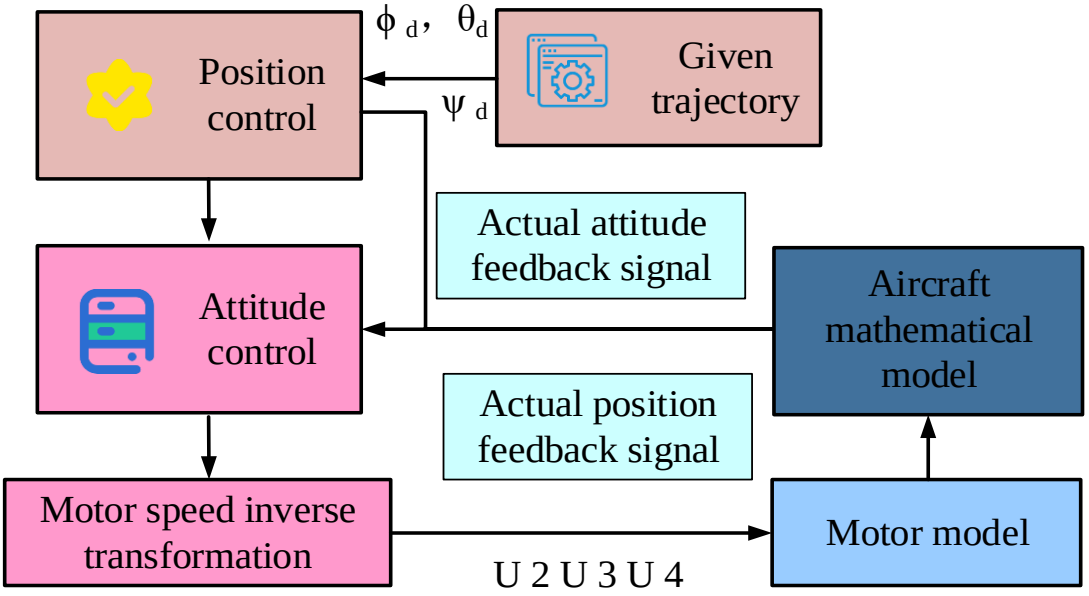

Fig. 3. PID control structure based on GA-PSO.

In Eq. (8), $u(t)$ is the input of the PID parameter vector. $e(t)$ is the error signal of PID control parameters. K_p, K_i, and K_d are the proportional gain, integral gain, and derivative gain of PID control parameters. Each individual input is subjected to fitness calculation, including sum of squared errors, overshoot, and response time, to achieve PID control performance evaluation, as shown in Eq. (9).

$$J = \int_0^T \left(e(t)^2 + \lambda_1 u(t)^2 + \lambda_2 \left(\frac{du(t)}{dt} \right)^2 \right) dt \tag{9}$$

In Eq. (9), J is the fitness function value. T is the total PID control time. λ_1 and λ_2 both represent weight factors. Following each iteration of the population update, an adaptive function is employed to assess the selected PID parameter solutions, thereby identifying the optimal control individual. This creates conditions for the next individual elimination and retention operations to improve the overall quality of the population. Based on the evaluation results of the adaptive function, the expression for selecting probabilities for each individual is given by Eq. (10).

$$P_i = \frac{J_i}{\sum_{j=1}^{N} J_j} \tag{10}$$

In Eq. (10), P_i and J_i are the selection probability and fitness of the current individual i. N means the population size. j is the individual in the population who is currently assigned a probability. To increase the diversity of the population and avoid getting stuck in local optima during algorithm solving, this study randomly selects gene fragments from any two individuals and performs crossover operations to generate new offspring individuals, as shown in Eq. (11).

$$\begin{cases} v^* = (v_1, \cdots, v_{k-1}, v_k, v_{k+1}, \cdots, v_n) \\ u^* = (u_1, \cdots, u_{k-1}, u_k, u_{k+1}, \cdots, u_n) \end{cases} \tag{11}$$

In Eq. (11), $u = (u_1, u_2, \cdots, u_n)$ and $v = (v_1, v_2, \cdots, v_n)$ are the generation of new individuals u^* and $v*$ after chromosome crossing between any two selected parental individuals. k is a random gene fragment cleavage point within the $1 \sim n$ range. Cross operation can increase population diversity, randomly mutate individuals, and further enhance the global nature of the algorithm, avoiding local optima. The random mutation operation performed on individuals is shown in Eq. (12).

$$x_k^* = \begin{cases} x_k + \Delta(t, U_{\max}^k - v_k), random(0,1) = 0 \\ x_k - \Delta(t, v_k - U_{\min}^k), random(0,1) = 1 \end{cases} \tag{12}$$

In Eq. (12), x_k is the individual's randomly selected cutting point for mutation. x_k* is the new mutation point generated after the mutation operation. $random(1,0)$ is a random integer representing the random value of the variance $\Delta(t, y)$. $[U_{\min}^k, U_{\max}^k]$ represents any cutting point within the range. The individual crossover mutation operation process is shown in Fig. 4.

In Fig. 4, by performing cross-mutation on individuals, the PID parameters of individuals can be randomly adjusted to obtain more global parameter solutions. The global advantage of GA has to some extent slowed down the computational speed of the algorithm. To deeply improve the calculation accuracy and velocity of the algorithm, the PSO algorithm is adopted for improvement. PSO is inspired by the foraging process of bird flocks and can accelerate the convergence process by updating particle velocity and position, and increase the accuracy of PID parameters to improve PID control performance. The velocity and location of particles are updated as shown in Eq. (13).

$$\begin{cases} x_i(0) = x_{\min} + rand(0,1) \times (x_{\max} - x_{\min}) \\ v_i(0) = v_{\min} + rand(0,1) \times (v_{\max} - v_{\min}) \end{cases} \tag{13}$$

In Eq. (13), $x_i(0)$ and $v_i(0)$ are the initial positions and velocities of the particles. $x_{\min} / x_{\max}$ and $v_{\min} / v_{\max}$ are the minimum and maximum values of particle position and velocity. PSO achieves further optimization of PID parameters by updating particle velocity and position, and the updated formula is shown in Eq. (14).

$$v_i(t+1) = \omega v_i(t) + c_1 r_1 (p_i - x_i(t)) + c_2 r_2 (g - x_i(t)) \tag{14}$$

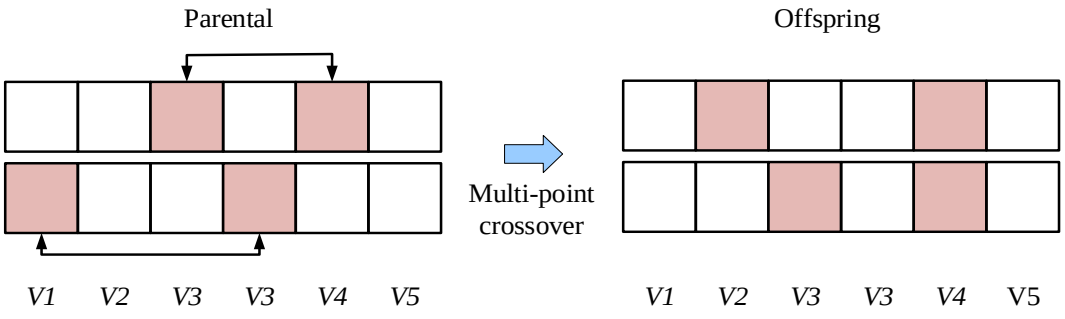

Fig. 4. Execution process of mutation operator.

In Eq. (14), $v_i(t+1)$ is the particle update speed. $v_i(t)$ is the velocity before particle update. ω denotes the inertia weight of particle velocity. c_1 and c_2 both represent learning factors. r_1 and r_2 are velocity weighting factors. p_i and g are velocity updates for particles. $x_i(t)$ is the optimal position for both the individual and the global. The formula for updating the particle's historical position based on its historical location and updated velocity is shown in Eq. (15).

$$x_i(t+1) = x_i(t) + v_i(t+1) \tag{15}$$

In Eq. (15), $x_i(t+1)$ is the current position of the particle after the position update. The schematic diagram of excavator trajectory planning is shown in Fig. 5.

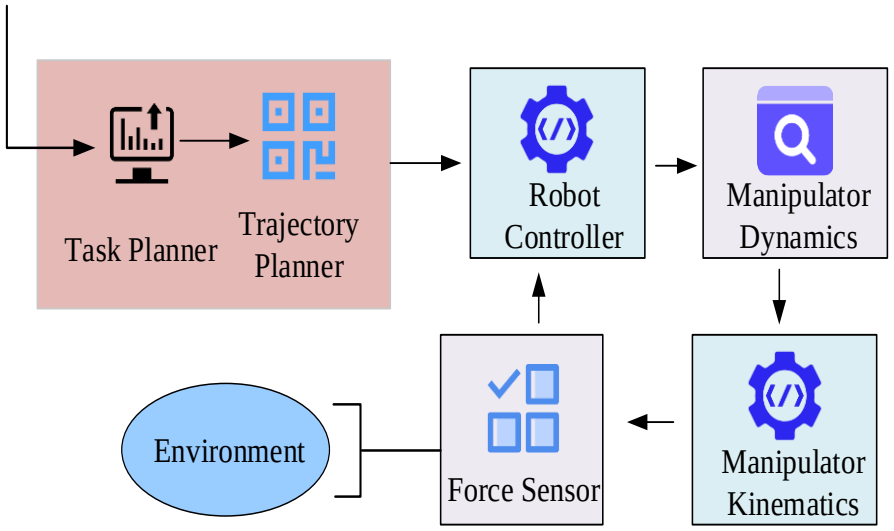

Fig. 5. Schematic diagram of excavator trajectory planning.

In Fig. 5, the process of mining mechanical trajectory planning is the process from task input to control instruction output.

IV. Results

Firstly, the anti-interference simulation model based on PID feedback control is tested to verify its control stability, accuracy, and error value. Next, the application effect of PID-MCS based on GA-PSO optimization is verified. The research method is compared in mining operation control under different working conditions to verify its superiority.

A. Performance Testing of PID Feedback Control for Anti-Interference Mining Trajectory Planning System

To validate the effectiveness of the constructed mining system dynamics simulation model, simulation experiments are conducted on the model. The hardware configuration used for the experimental equipment is Genuine Intel ®CPU 2140 (dual-core) 1.6GHz, 512MB of memory. The experiment is conducted on the MATLAB 7.0 platform. In MATLAB, a 3D simulation model of the linkage coordinates of the RA in the mining system is constructed based on the improved D-H parameters. The simulation experiment is conducted on a scaled-down testing platform to simulate the motion and operation process of the RA in a real environment, creating conditions for the structural and operational analysis of the RA. Table I shows the D-H parameters.

Firstly, the effectiveness of FIOM in controlling the motion of RAs is experimentally verified, using three, five, and nine iterations as comparisons. Each interpolation method is applied to joints 1, 2, and 3 of the RA. The joint motion fluctuation curve over time is used as the evaluation index, as displayed in Fig. 6. In Fig. 6, different numbers of interpolation methods have a good constraint effect on the motion path of the RA, with smooth and continuous curves without significant fluctuations. In Fig. 6 (a), the cubic interpolation method has the worst constraint effect on the motion process of the RA, with significant fluctuations occurring at both the beginning and end of the RA motion. In Fig. 6 (b), FOIM has the best constraint effect with no significant fluctuations, and the curve remains within the range of [-0.25, 0.25]. In Fig. 6 (c) and (d), the seven-degree and nine-degree interpolation methods improved the constraint performance by 2% and 3% respectively based on five degrees, but these two methods have higher energy consumption. This indicates that FOIM can ensure higher constraint performance while also being more energy-efficient.

To further verify the anti-interference ability of the path planning system after adopting the PID controller, the prediction and actual trajectory error of the RA are used as evaluation indicators, as shown in Fig. 7. In the trajectory prediction of four joints using the proposed method, the error is within 5% compared to the true values, and the motion trajectory curves are smooth, continuous, and without significant abrupt changes. In Fig. 7 (a), the application effect in joint 1 is the worst, with a predicted and actual displacement difference of 0.4m. In joint 2 of Fig. 7 (b), the actual and predicted displacement values have the highest overlap, with a difference of less than 0.1m. In Fig. 7 (c) and (d), the error values of joint 3 and joint 4 are at an intermediate level, within 0.3m. The proposed method can overcome the influence of nonlinear factors in the real environment when applied to MCS and has high feasibility and accuracy.

TABLE I. IMPROVED D-H COORDINATE PARAMETERS

Joint	Joint angle/°	Z-axis offset/mm	X-axis offset/mm	Rotation angle around the X-axis	Range of variation
1	-90°~90°	0	59	734	2643mm
2	-34.6°~76.2°	0	3680	0	2677mm
3	0°	136	1734	0	-40°~40°
4	0°	180	1046	0	3000

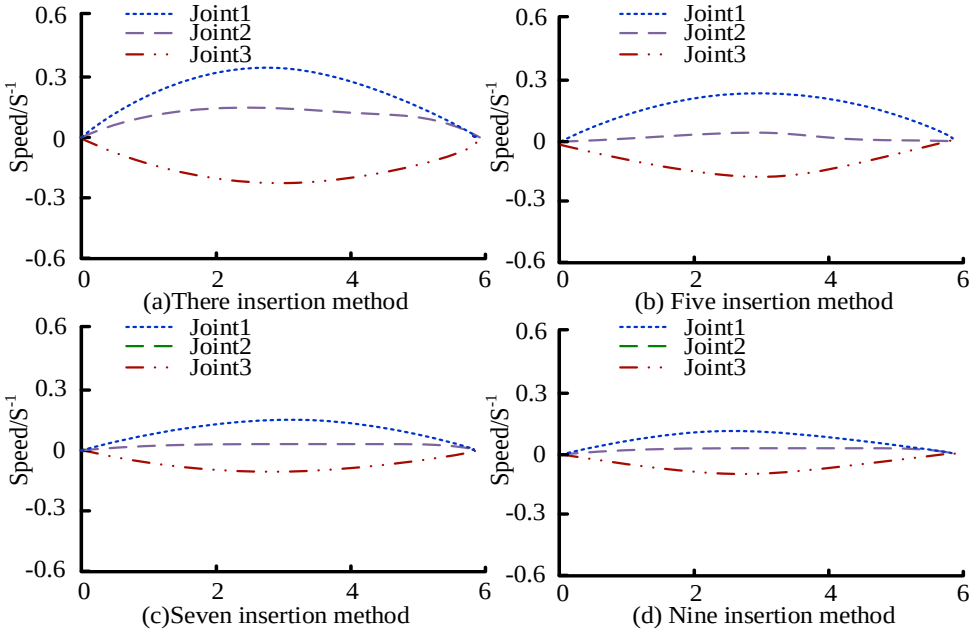

Fig. 6. Comparison of motion speed curves under different interpolation modes.

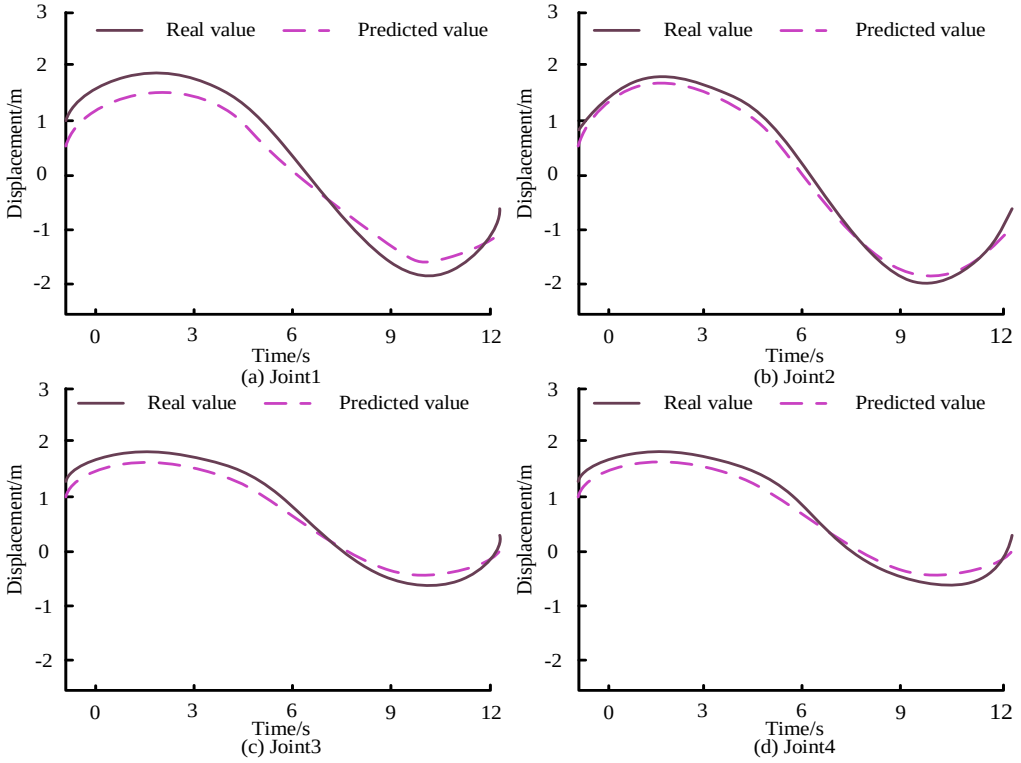

Fig. 7. Performance test under PID control of RA.

B. Application Verification of PIDMCS based on GA-PSO Optimization

After verifying the performance of the PID-controlled RA simulation model in the previous section, the actual application effect of the PID controller optimized by GA-PSO is analyzed. The displacement and pressure curves of the hydraulic cylinder applied to the practical application scenario of the bucket hydraulic cylinder using the research method are shown in Fig. 8. During the bucket operation, it can move accurately by the pre-set trajectory, and the displacement and pressure curves always show stability. In Fig. 8 (a), the displacement curve of the bucket cylinder encounters obstacles and evades them at 8-11s, and then returns to normal track operation. In Fig. 8 (b), there is consistency in the action of the pressure changes in the large and small chambers of the bucket cylinder at time points 2s, 4s, 8s, 12s, and 18s. The pressure curve exhibits symmetry within the ranges of [2, 4], [4, 8], [8, 12], and [18, 24]. The proposed excavation trajectory control method has good stability and accuracy in controlling the pressure parameters of the hydraulic system and can make the excavator move smoothly according to the predetermined track in practical applications.

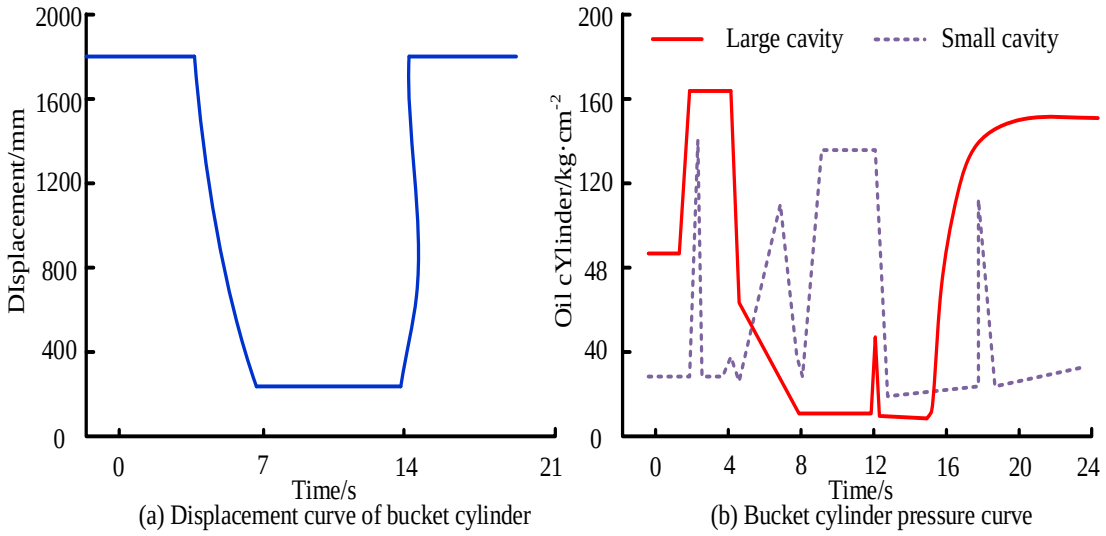

(a) Displacement curve of bucket cylinder (b) Bucket cylinder pressure curve

Fig. 8. Displacement and pressure control curve of bucket cylinder.

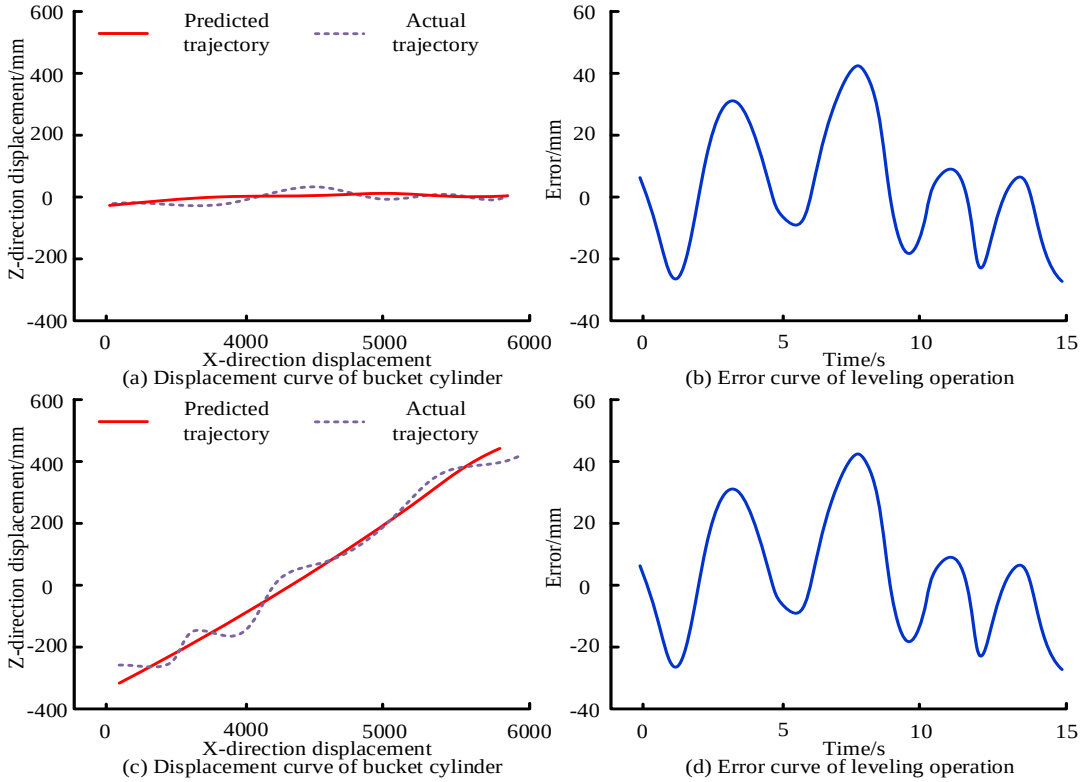

(a) Displacement curve of bucket cylinder (b) Error curve of leveling operation

(c) Displacement curve of bucket cylinder (d) Error curve of leveling operation

Fig. 9. Trajectory control curves for different work environments.

To further verify the control effect during bucket excavation, the motion trajectory of the bucket during leveling and slope operations is tracked. Fig. 9 shows the error result between the calculated actual value and the predicted value. In Fig. 9 (a) and (b), the trajectory and error curve of the bucket tooth tip indicate that the maximum error in horizontal displacement is 44.21mm. In Fig. 9 (c) and (d), the maximum error of water diagonal displacement during bucket slope operation is 41.41mm. Overall, the motion errors are within a reasonable range, and the motion curve is smooth, continuous, and without significant fluctuations. The proposed method can ensure stable and accurate control effects in two different operating environments, with errors controlled within a reasonable range, and the results have high reliability.

To further verify the practical application effect of GA-PSO in optimizing PID parameters and mining trajectory planning systems, three classic algorithms, Adaptive Genetic Algorithm (AGA), A* Search Algorithm (A*), and Rapidly-exploring Random Tree (RTT), are compared. Fig. 10 shows the results of using the convergence accuracy and rate of the algorithm as performance evaluation indicators. As the number of iterations increases, the convergence accuracy and rate of the proposed algorithm are better than the other three compared algorithms. In Fig. 10 (a), the proposed algorithm converges to 0.05 after 50 iterations, while AGA, A*, and RTT algorithms converge to similar levels after 80, 91, and 110 iterations, respectively. The average convergence rate of the three algorithms is 0.08 lower than the proposed algorithm. In Fig. 10 (b), the proposed algorithm achieves the highest accuracy of 94%, while AGA has the lowest accuracy of only 75%. The accuracy of A * and RTT algorithms is at an intermediate level, which is 15.3% and 17.5% lower than the proposed algorithm. Therefore, the GA-PSO has the best accuracy and efficiency when applied to mining trajectory planning systems.

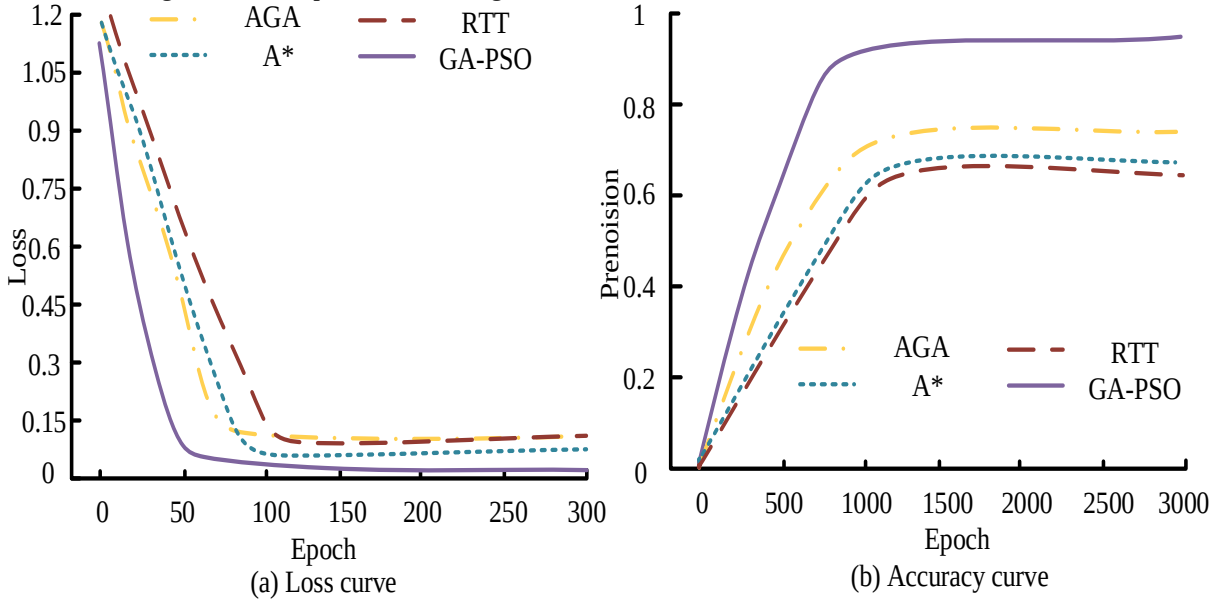

Fig. 10. Comparison of convergence accuracy and efficiency of different algorithms.

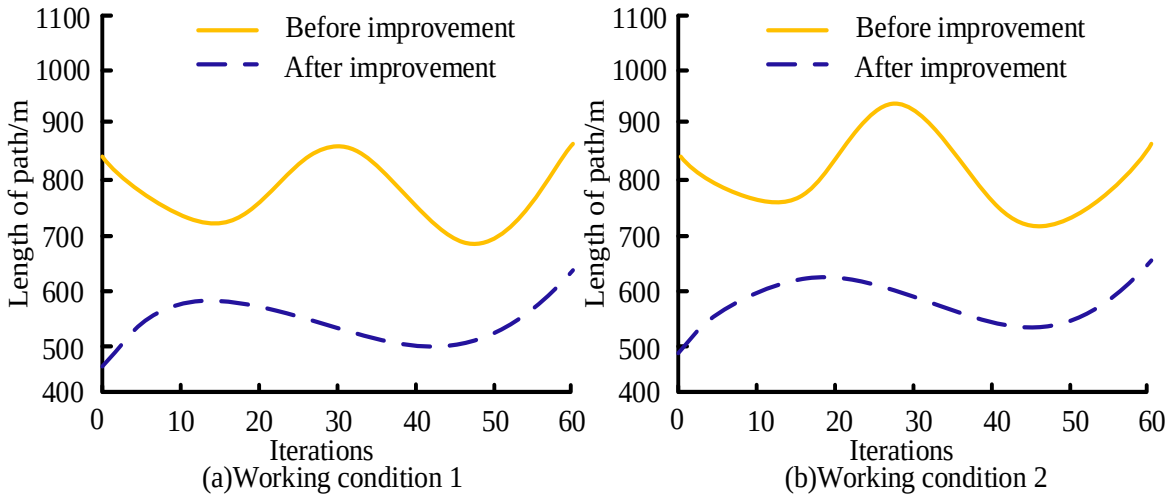

Fig. 11. Comparison of algorithm path planning length before and after improvement.

To test the path planning performance of the research algorithm, it is tested under two different load levels and compared with the improved algorithm using path length as the evaluation index, as exhibited in Fig. 11. Overall, the path length of the improved algorithm is shorter. In condition 1 of Fig. 11 (a), the longest path of the algorithm before improvement is 884m at 30 iterations, which is 46.2% longer than the improved algorithm. In condition 2 of Fig. 11 (b), the improved algorithm has a maximum path of 962m at 60 iterations, a decrease of 43.5% compared to before the improvement. In two different levels of complexity, the error is within 5%, indicating that the improved method has high reliability and accuracy.

V. Discussion

The proposed ECT-based ICS shows obvious performance improvement in the application of large-scale mining excavators by combining the PID controller optimized by GA-PSO technology. The analysis of experimental results demonstrates that the enhanced PID feedback control method exhibits superior comprehensive performance in search performance and convergence speed when compared to traditional PID control technology, fuzzy control, and the use of GA and PSO in isolation. In the aspect of the anti-interference ability, the proposed method effectively improves the robustness of the excavator in the face of internal and external interference through adaptive adjustment of the PID controller. This is reflected in the stability of the displacement and pressure curve of the hydraulic cylinder. The stability and symmetry of the curve show the precise control ability of the system in actual operation [20, 21]. In addition, the trajectory prediction error is controlled within 5%, which further proves the high reliability and adaptability of the system in complex mine environments.

In terms of optimization efficiency, the application of the GA-PSO algorithm significantly improves the accuracy and speed of parameter optimization. A comparative analysis of the algorithms reveals that the proposed algorithm rapidly converges to 0.05 after 50 iterations, with an accuracy of 94%, which is superior to the other three classical algorithms [11-13]. This shows that the GA-PSO algorithm can balance the efficiency of global search and local search more effectively when dealing with complex trajectory planning problems.

VI. Conclusion

Aiming at the intelligent control of large mining equipment in complex mine environments, this paper proposes an ICS based on ECT. Through the PID controller optimized by combining GA and PSO technology, the accuracy, response speed, and robustness of the control system are improved. The experimental results showed that the control system had good stability and accuracy under different working conditions. The trajectory prediction error was controlled within 5%, the displacement and pressure curves of the hydraulic cylinder were stable, and the algorithm converged rapidly after 50 iterations, with an accuracy of 94%. These results proved the effectiveness of the proposed method and provided a practical solution for improving the intelligent control performance of large mining equipment.

Nevertheless, the research is not without limitations. In particular, the comprehensive control performance of the algorithm requires further improvement in a more complex actual mine environment. Future research will concentrate on enhancing the algorithm's adaptability to more effectively address the evolving mine environment. Additionally, more efficient optimization strategies will be investigated to minimize calculation time and enhance control accuracy. In addition, advanced technologies such as DL are considered to be integrated into the control system to further improve the level of intelligent control.

References

[1] Liu Y, Cao B, Li H. Improving ant colony optimization algorithm with epsilon greedy and Levy flight. Complex & Intelligent Systems,2021 ,7(4):1711-1722.

[2] Stodola P. Hybrid ant colony optimization algorithm applied to the multi-depot vehicle routing problem. Natural computing, 2020 ,19(2):463-475.

[3] Deng W, Xu J, Song Y, Zhao H. An effective improved co-evolution ant colony optimisation algorithm with multi-strategies and its application. International Journal of Bio-Inspired Computation, 2020, 16(3):158-170.

[4] Li W, Wang GG, Gandomi AH. A survey of learning-based intelligent optimization algorithms. Archives of Computational Methods in Engineering, 2021 ,28(5):3781-3799.

[5] Wellendorf A, Tichelmann P, Uhl J. Performance Analysis of a Dynamic Test Bench Based on a Linear Direct Drive. Archives of Advanced Engineering Science, 2023, 1(1):55-62.

[6] Sadiq A T, Raheem F A, Abbas N. Ant colony algorithm improvement for robot arm path planning optimization based on D strategy. International Journal of Mechanical & Mechatronics Engineering, 2021, 21(1): 196-111.

[7] Wellendorf A, Tichelmann P, Uhl J. Performance Analysis of a Dynamic Test Bench Based on a Linear Direct Drive. Archives of Advanced Engineering Science, 2023, 1(1):55-62.

[8] Kanso B, Kansou A, Yassine A. Open capacitated ARC routing problem by hybridized ant colony algorithm. RAIRO-Operations Research, 2021, 55(2): 639-652.

[9] Wang Z, Ding H, Li B, Bao L, Yang Z, Liu Q. Energy efficient cluster based routing protocol for WSN using firefly algorithm and ant colony optimization. Wireless Personal Communications, 2022, 125(3): 2167-2200.

[10] Sohail A. Genetic algorithms in the fields of artificial intelligence and data sciences. Annals of Data Science, 2023 , 10(4):1007-1018.

[11] Too J, Abdullah A R. A new and fast rival genetic algorithm for feature selection. The Journal of Supercomputing, 2021, 77(3): 2844-2874.

[12] Gad AG. Particle swarm optimization algorithm and its applications: a systematic review. Archives of computational methods in engineering, 2022 ,29(5):2531-2361.

[13] Pervaiz S, Bangyal WH, Ashraf A, Nisar K, Haque MR, Ibrahim A, Ag AB, Chowdhry B, Rasheed W, Rodrigues JJ. Comparative research directions of population initialization techniques using PSO algorithm. Intelligent Automation & Soft Computing, 2022 ,32(3):1427-1444.

[14] Zhang H, Thompson J, Gu M, Jiang XD, Cai H, Liu PY, Shi Y, Zhang Y, Karim MF, Lo GQ, Luo X. Efficient on-chip training of optical neural networks using genetic algorithm. Acs Photonics, 2021 , 8(6):1662-1672.

[15] Minh HL, Khatir S, Rao RV, Abdel Wahab M, Cuong-Le T. A variable velocity strategy particle swarm optimization algorithm (VVS-PSO) for damage assessment in structures. Engineering with Computers, 2023 ,39(2):1055-1084.

[16] Pozna C, Precup RE, Horváth E, Petriu EM. Hybrid particle filter–particle swarm optimization algorithm and application to fuzzy controlled servo systems. IEEE Transactions on Fuzzy Systems, 2022 ,30(10):4286-4297.

[17] Shishavan ST, Gharehchopogh FS. An improved cuckoo search optimization algorithm with genetic algorithm for community detection in complex networks. Multimedia Tools and Applications, 2022 , 81(18):25205-25231.

[18] Chotikunnan P, Chotikunnan R. Dual design PID controller for robotic manipulator application. Journal of Robotics and Control (JRC), 2023 ,4(1):23-34.

[19] Saleh B, Yousef AM, Ebeed M, Abo-Elyousr FK, Elnozahy A, Mohamed M, Abdelwahab SA. Design of PID controller with grid connected hybrid renewable energy system using optimization algorithms. Journal of Electrical Engineering & Technology, 2021 ,16(6):3219-3233.

[20] Suseno EW, Ma'arif A. Tuning of PID controller parameters with genetic algorithm method on DC motor. International Journal of Robotics and Control Systems, 2021 ,1(1):41-53.

[21] Ma'arif A, Setiawan NR. Control of DC motor using integral state feedback and comparison with PID: simulation and arduino implementation. Journal of Robotics and Control (JRC), 2021, 2(5):456-461.

[22] Lin P, Wu Z, Fei Z, Sun XM. A generalized PID interpretation for high-order LADRC and cascade LADRC for servo systems. IEEE Transactions on Industrial Electronics, 2021 ,69(5):5207-5214.

[23] Kristiyono R, Wiyono W. Autotuning fuzzy PID controller for speed control of BLDC motor. Journal of Robotics and Control (JRC), 2021 ,2(5):400-407.

[24] Nath UM, Dey C, Mudi RK. Review on IMC-based PID controller design approach with experimental validations. IETE Journal of Research, 2023 ,69(3):1640-1660.

[25] UsmanA M, Abdullah M K. An Assessment of Building Energy Consumption Characteristics Using Analytical Energy and Carbon Footprint Assessment Model. Green and Low-Carbon Economy, 2023, 1(1): 28-40.